Characterization of Oligomers of AlCl: Al–Cl versus Al–Al Bonding

Hans-Jörg Himmel*[a]

Keywords: Subvalent compounds / Aluminium / Reaction mechanisms / Matrix isolation / Quantum chemical calculations

Oligomers of AlCl have been characterized. By using the matrix isolation technique, the dimer Al_2Cl_2, which exhibits a D_{2h}-symmetric ring structure, was generated in significant quantities and analyzed by its IR and Raman spectra in combination with quantum chemical calculations. The structures of the trimer and tetramer have also been evaluated. A surprising result is that the minimum energy structure of the trimer (C_s symmetry) features direct Al–Al bonds, two terminal Al–Cl bonds, and one bridging Cl atom. A weak, isotopically structured IR band can be assigned to the antisymmetric ν(Al–Cl_t) mode of this trimer (Cl_t denotes a terminal Cl atom). The enthalpy change for each of the oligomerization steps has been calculated. For the dimerization of AlCl to give Al_2Cl_2, the Gibbs energy change was calculated as a function of temperature at different pressures. It turns out that neither the Al_2Cl_2 dimer nor any higher oligomers are present in significant quantities in the gas phase, at least under the conditions of the experiments. The thermodynamic properties show that matrix isolation represents the optimal method of generating and characterizing these species. On the basis of the experimental results the barrier for dimerization of AlCl should be next to zero.

Introduction

AlCl is an interesting example of a very simple compound featuring Al in the formal oxidation state +1. Several possibilities for generating the molecule have been discussed.[1] These include the reaction of Al with $AlCl_3$, and the reaction of Al with HCl, both requiring high temperatures since AlCl is thermodynamically stable only at high temperatures and disproportionates to Al metal and $AlCl_3$ at lower temperatures. The temperature minimum needed for the generation depends, of course, on the pressure, e.g. under high vacuum (10^{-5} mbar) temperatures around 1250 K or more are needed to generate AlCl in the almost complete absence of $AlCl_3$. The monomer AlCl has already been studied intensively both in the gas phase[2–5] and in inert gas matrices (Figure 1).[6,7] Information about the compound in the solid phase and in solution is, however, sparse.[8]

By using a cocondensation technique and a mixture of solvents, it is possible to obtain metastable solutions of AlCl,[1] which have been used extensively for the preparation of new cluster compounds.[1,9] NMR spectroscopic studies[10] clearly show that the calculated chemical shift of the isolated AlCl molecule (δ = +150 ppm) does not match the position of the NMR signal observed for such solutions (δ = +35 ppm). The calculated NMR spectrum of the tetramer Al_4Cl_4 (δ = +235 ppm) is also not consistent with the experimentally observed spectrum. These results indicate a relatively strong solvent effect, and the AlCl molecules or, more likely, oligomers are coordinated by one or more solvent molecules. However, the exact composition still remains unknown.

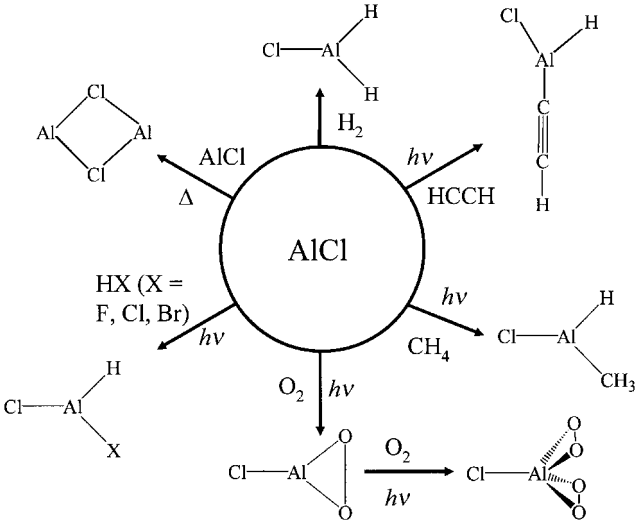

Figure 1. Known reactions of photoactivated AlCl molecules as studied in matrix isolation experiments.

Matrix isolation studies have permitted the reactivity of AlCl monomers to be assessed in some detail. AlCl in its ground electronic state ($^1\Sigma$) is not very reactive. Thus, no spontaneous reaction occurs with O_2 under the conditions of matrix experiments.[11] Only when O atoms are generated is reaction possible, which leads to OAlCl.[12] Photoactivated AlCl reacts, on the other hand, not only with O_2,[11]

[a] Institut für Anorganische Chemie, Universität Karlsruhe, Engesserstr., Geb. 30.45, 76180 Karlsruhe, Germany
Fax: +49-721-608-4854
E-mail: himmel@chemie.uni-karlsruhe.de

  DOI: 10.1002/ejic.200401016

but also readily with molecules such as CH_4,[13] H_2,[14] C_2H_2[15] and HX (X = F, Cl or Br).[16] The effect of photolysis has been shown to lead to excitation of an electron from a σ to a π orbital with strong p character localized mainly at the Al atom.[17] The reaction products are all Al^{III} species that are formed exothermally. Figure 1 summarizes the photoactivated reactions and their products which have been studied so far.

The dimer $[AlCl]_2$ had been sighted previously in matrix isolation experiments. Thus, a band at 270 cm^{-1} in the IR spectrum of AlCl that was isolated in an Ar matrix had been assigned to this dimer.[1] However, few details were given, and the fine structure that the band might be expected to show (see the results of this work) was not resolved. Here it will be shown with the aid of higher-resolution IR spectra that this band corresponds to two vibrational modes, each showing the isotopic splitting characteristic of two chemically equivalent Cl atoms in the molecule. In addition, Raman spectra will be reported for the first time, giving clear evidence of one of the $\nu(a_g)$ modes of the dimer. Theoretical studies of $[AlCl]_2$[18] predict a molecule that exhibits a planar, D_{2h}-symmetric structure for its global energy minimum. The experimentally measured frequencies will be used to estimate the bond angles in this ring.

Somewhat surprisingly, no experimental or theoretical information about the trimer Al_3Cl_3 has been available hitherto. Here, the structure of this molecule will be analyzed, and a weak, isotopically structured band in the IR spectrum can tentatively be assigned to it. The tetramer Al_4Cl_4 has been calculated previously,[10,24] and was shown to exhibit a tetrahedral structure with Al–Al and Al–Cl distances of 259.8–263.9 and 209.8–210.9 pm, respectively. Knowledge of the structure and bonding of $[AlCl]_n$ oligomers is desirable in order to anticipate possible structures for solid AlCl. So far, it has proved impossible to characterize the structure of this solid in a more than qualitative way.[8]

Results

IR Spectra

Figure 2a shows the IR spectrum measured for AlCl that was isolated in an Ar matrix. An intense absorption with a doublet pattern occurs at 455.1/449.8 cm^{-1}, as previously assigned to the AlCl monomer. The doublet pattern arises from the presence of the two isotopomers $Al^{35}Cl$ and $Al^{37}Cl$. Two weaker absorptions at high wavenumbers, 462.3 and 459.0 cm^{-1}, also exist. Besides these strong absorptions due to AlCl monomers, the spectrum presents a structured feature at 270 cm^{-1}, which clearly shows several maxima. The structure of the band can be seen in more detail in the higher-resolution spectrum illustrated in Figure 2b.

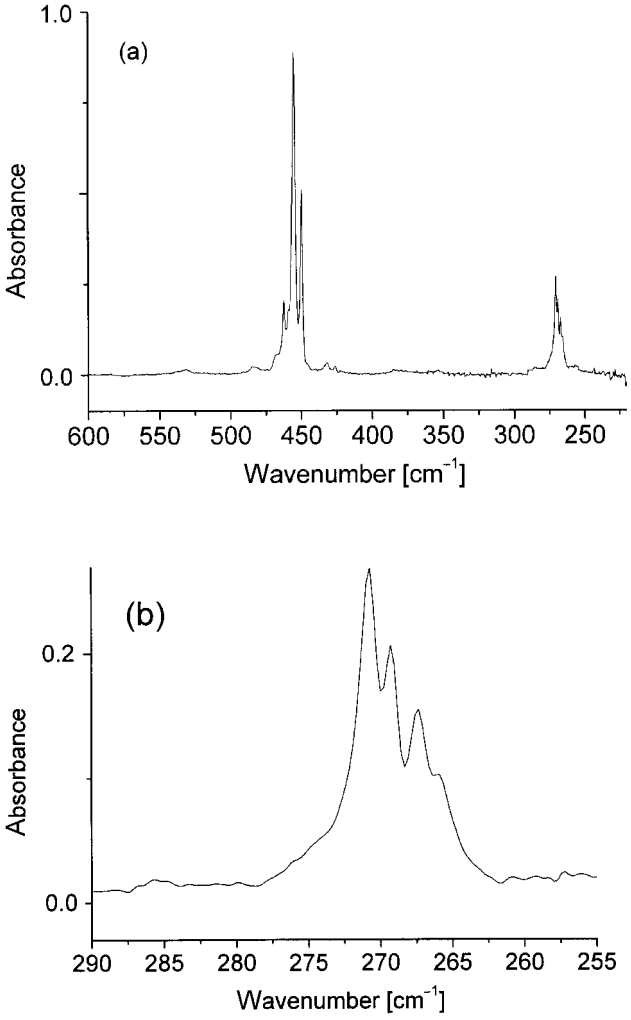

Figure 2. (a) IR spectrum of an Ar matrix containing AlCl vapour. (b) Detailed spectrum of the region around 270 cm^{-1}.

In addition to these intense absorptions, the IR spectrum gives evidence for a weak band, and its maximum is located at 531.3 cm^{-1} (see Figure 3). On the low-energy side of this band, two secondary maxima are visible (at 528.8 and 526.4 cm^{-1}), which are most likely to be due to the presence of different $^{35}Cl/^{37}Cl$ isotopomers.

Raman Spectra

Raman measurements were made to obtain further information. A typical spectrum is displayed in Figure 4a. The ν(Al–Cl) mode of the AlCl monomer near 450 cm^{-1} is clearly visible with the doublet pattern typical for the presence of a single Cl atom in the carrier. Another signal appears with a maximum at 298.6 cm^{-1}. Experiments with varying concentrations of AlCl in the matrix indicate that this signal belongs to the same species as the band near 270 cm^{-1} in the IR experiments.

Discussion

We start this section with a characterization of $[AlCl]_n$ oligomers (n = 1–4) on the basis of the experimental data

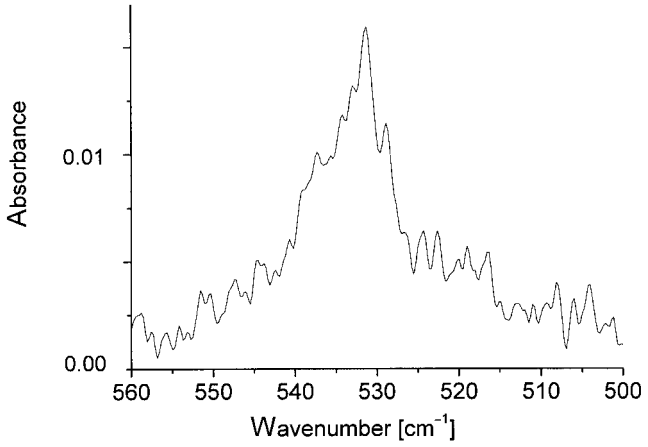

Figure 3. Higher-resolution IR spectrum in the region around 530 cm^{-1}.

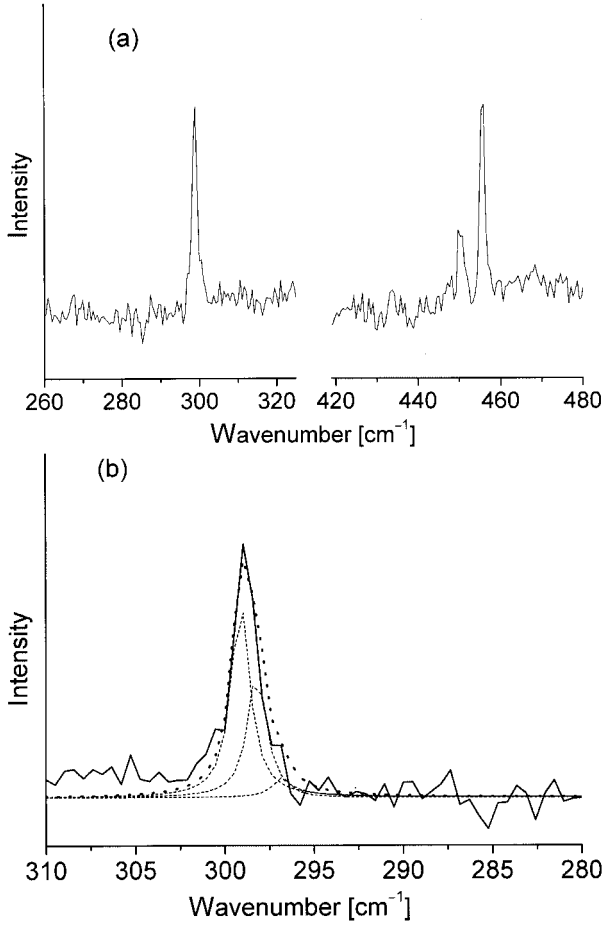

Figure 4. Raman spectra obtained for AlCl isolated in an Ar matrix. (a) In the region of the AlCl monomer and the Al_2Cl_2 dimer. (b) Comparison between the observed signal for the dimer and a fit on the basis of the presence of ^{35}Cl and ^{37}Cl in their natural abundances (see Discussion).

and the results from the quantum chemical calculations. There follows a discussion of the oligomerization process, which considers the enthalpy and Gibbs energy changes for the initial oligomerization reactions.

AlCl

The experimental data indicate that the AlCl monomer is the dominant guest species in the Ar matrices. According to our calculations and with the use of BP/SVP, the Al–Cl distance in the $^1\Sigma$ ground electronic state is 216.4 pm; MP2/TZVPP predicts a value of 215.1 pm. These results are in very good agreement not only with those calculated previously (213–216 pm),[19,20,24] but also with the well-defined experimental estimate (213.0 pm).[2] The IR band at 455.1/449.8 cm^{-1} has already been assigned to the AlCl monomer; the doublet pattern arising from the presence of the two isotopomers $Al^{35}Cl$ and $Al^{37}Cl$. The weaker extra doublet at 462.3/459.0 cm^{-1} also belongs to AlCl, in all probability. This component, shifted by 7.3 cm^{-1} from the main absorption, may well be due to the occupation of a different matrix site. The harmonic wavenumber is predicted to be 476.8 cm^{-1} according to BP/SVP, and 482.1 cm^{-1} according to MP2/TZVPP calculations. The calculated wavenumber is in good agreement with the experimental value of ω_e = 481.30 cm^{-1} for the gaseous molecule.[2,5] The anharmonicity $\omega_e x_e$ was previously determined to be 1.95 cm^{-1}.[5] As expected, a polar molecule like AlCl is subjected to a significant matrix shift (cf. InCl).[21] Analogies between compounds in the two series BF, AlF, AlCl and CO, SiO, SiS have already been discussed in detail.[22]

$[AlCl]_2$

There can be little doubt that the band at around 270 cm^{-1} visible in the IR spectrum can be assigned to an oligomer of AlCl, $[AlCl]_n$. The higher-resolution IR spectrum (see Figure 2a) shows a fine structure within the band which is caused by different isotopomeric forms and allows one to determine, with some confidence, the exact composition of the species. Inspection of the fine structure shows immediately that it cannot be explained by the isotopic pattern of a single mode, but must originate from two different modes with only slightly different wavenumbers. Attempts have been made to simulate the isotopic pattern on the basis of the presence of two Cl atoms in the molecule (with relative natural abundances of 75.8:24.2 for the ^{35}Cl and ^{37}Cl isotopes). In total, six Lorenz-type curves are thus involved in this fit. Figure 5 compares the simulated spectrum with that experimentally observed.

The three Lorentz-type curves of the first mode (which exhibit relative intensities of 57.5:36.7:5.8 reflecting the relative natural abundance of ^{35}Cl and ^{37}Cl) have their maxima at wavenumbers of 270.95, 269.29 and 267.51 cm^{-1}. The three Lorenz curves of the second mode, with the same relative intensities, are located at 267.24, 265.70 and 264.54 cm^{-1}. It can be seen that the simulated spectrum is in good agreement with that observed, a result appearing to confirm the presence of two equivalent Cl atoms in the molecule.

As already mentioned, the experiments give every reason to assume that the signal in the Raman spectrum with its maximum at 298.6 cm^{-1} belongs to the same molecule. Al-

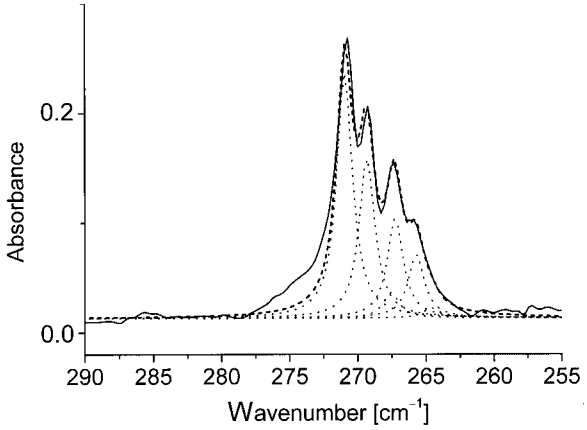

Figure 5. Experimental IR spectrum of $(AlCl)_2$ and fit on the assumption of the presence of two different modes, each with three isotopic components ($^{35}Cl^{35}Cl$, $^{35}Cl^{37}Cl$, and $^{37}Cl^{37}Cl$, in their natural abundances).

though the resolution of the Raman spectra (0.5 cm^{-1}) is unfortunately clearly insufficient to resolve any fine structure of this signal, the profile can be modeled with three Lorenz-type curves. Figure 3b shows the observed signal together with the simulation, again assuming the presence of two chemically equivalent Cl atoms. It can therefore be concluded that this species is most likely to be the dimer Al_2Cl_2.

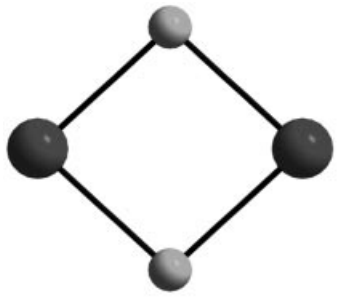

$[AlCl]_2$

Table 1 summarizes the results of quantum chemical calculations on the dimer Al_2Cl_2. According to these calculations, the Al–Cl distance in the dimer is slightly longer than in the AlCl monomer (246.8 versus 216.3 pm). The Cl–Al–Cl and Al–Cl–Al angles are 84.7° and 95.3°, respectively, so that the Al atoms are separated by 364.8 pm. In Table 2, the wavenumbers calculated with BP/SVP are compared with those observed. The general level of agreement is very pleasing. The calculations also give an explanation of why the Raman spectra give evidence for the $\nu_1(a_g)$ mode, but not for the other two modes with *gerade* symmetry.

The Raman intensity calculated for $\nu_1(a_g)$ is more than four times larger than those calculated for $\nu_2(a_g)$ or $\nu_5(b_{3g})$.

It is worth mentioning that the difference in wavenumbers measured between the ν_3 and ν_4 modes of $Al(^{35}Cl)(^{37}Cl)Al$ is not the same as that between the corresponding modes of the $Al(^{35}Cl)_2Al$ and $Al(^{37}Cl)_2Al$ isotopomers. In the case of the ν_3 mode, for example, the $^{35}Cl^{37}Cl$ isotopomer has a wavenumber which is 1.54 cm^{-1} lower than that of the $^{35}Cl^{35}Cl$ isotopomer, but only 1.16 cm^{-1} higher than that of the $^{37}Cl^{37}Cl$ isotopomer. For the ν_4 mode, the situation is reversed, and the difference in wavenumbers from the $^{35}Cl^{37}Cl$ isotopomer is smaller for the $^{35}Cl^{35}Cl$ isotopomer (1.66 cm^{-1}) than for the $^{37}Cl^{37}Cl$ isotopomer (1.78 cm^{-1}). This observation can be explained as a consequence of the symmetry reduction from D_{2h} to C_{2v} in the $^{35}Cl^{37}Cl$ isotopomer. Because of this reduction, the symmetry of the modes changes [$\nu_1(a_g) \rightarrow \nu_1(a_1)$, $\nu_2(a_g) \rightarrow \nu_2(a_1)$, $\nu_3(b_{1u}) \rightarrow \nu_3(b_1)$, $\nu_4(b_{2u}) \rightarrow \nu_4(a_1)$, $\nu_5(b_{3g}) \rightarrow \nu_5(b_1)$, $\nu_6(b_{3u}) \rightarrow \nu_6(b_2)$]. In D_{2h} symmetry, the ν_3 and ν_4 modes belong to two different irreducible representations, b_{1u} and b_{2u}, respectively. There are no other modes with the same symmetry so that neither mode suffers any coupling. In the case of $Al(^{35}Cl)(^{37}Cl)Al$ with C_{2v} symmetry, however, the modes belong to the irreducible representations b_1 and a_1, respectively. The mode ν_5 now also belongs to b_1, and ν_1 and ν_2 belong to a_1. Since the wavenumber calculated for ν_5 (131.6 cm^{-1}) is close to that measured for ν_3 (269.29 cm^{-1}), and that observed for ν_1 (297.7 cm^{-1}) is even closer to that observed for ν_4 (265.70 cm^{-1}), mode coupling is expected to be significant between these two pairs of vibrations. The coupling between ν_3 and ν_5 must lead to an increase in the wavenumber of ν_3 (and a decrease in the wavenumber for ν_5). In the same vein, the coupling between ν_1 and ν_4 must lead to an increase in the wavenumber of ν_1 and a decrease in that of ν_4. This mode coupling is responsible for the wavenumber shifts displayed by the bands caused by $Al(^{35}Cl)(^{37}Cl)Al$, which do not fall midway between the positions of the corresponding modes of $Al(^{35}Cl)(^{35}Cl)Al$ and $Al(^{37}Cl)(^{37}Cl)Al$. The behaviour is thus a good indication that the molecule is, as suggested by the calculations, planar and of high symmetry (D_{2h}).

It should also be mentioned that the angles Cl–Al–Cl and Al–Cl–Al can be estimated purely on the basis of the IR spectra measured for the different isotopomers. In D_{2h} symmetry, the b_{1u} and b_{2u} fundamentals are each unique and do not couple with other modes. The G matrix element for b_{1u}, $G_S(b_{1u})$ (where S denotes G with respect to symmetry coordinates), is as follows:

$$G_S(b_{1u}) = \mu_{Al}(1 + \cos\alpha) + \mu_{Cl}(1 + \cos\alpha) \propto \nu_3^2$$

(α is the Cl–Al–Cl angle and μ_{Al} and μ_{Cl} the inverse masses of Al and Cl, respectively). The corresponding $G_S(b_{2u})$ element is:

$$G_S(b_{2u}) = \mu_{Al}(1 + \cos\alpha) + \mu_{Cl}(1 + \cos\alpha) \propto \nu_4^2$$

This implies that the ratio of ν_4 measured for the two isotopomers $[Al^{35}Cl]_2$ and $[Al^{37}Cl]_2$ is independent of the Cl–Al–Cl angle and should be 1.0120. On the other hand, the corresponding ratio of the ν_3 modes varies with the Cl–Al–Cl angle. The experimental ratios are 1.0129 and 1.0102 for ν_3 and ν_4, respectively. In the event of angles of 90°, the two ratios should be identical. From the experimental data, Cl–Al–Cl and Al–Cl–Al angles of 95° and 85°, respectively, can be calculated. Thus the angles are indeed close to 90° (the error caused by the fit of the experimental curve and the neglect of anharmonicity effects might be about 8°),

Table 1. Calculated geometric parameters (bond lengths in pm, angles in °), vibrational properties (wavenumbers in cm^{-1}, IR intensities in $km\,mol^{-1}$ given in parentheses, RA intensities relative to the most intense signal in the case of BP/aug-cc-pVTZ) and energy (in hartree) for Al_2Cl_2 (D_{2h} symmetry).

	BP/SVP	MP2/TZVPP	BP/aug-cc-pVTZ
Al–Cl	246.8	243.8	247.2
Al···Al	364.8	361.3	363.0
Cl–Al–Cl	84.7	84.4	85.5
Al–Cl–Al	95.3	95.6	94.5
$\nu_1(a_g)$	298.4 (0)	303.7 (0)	286.8 (IR:0, RA: 100)
$\nu_2(a_g)$	164.0 (0)	176.6 (0)	160.0 (IR: 0, RA:22)
$\nu_3(b_{1u})$	287.1 (311)	292.0 (340)	281.8 (IR: 267, RA: 0)
$\nu_4(b_{2u})$	277.8 (59)	285.2 (84)	265.9 (IR: 76, RA: 0)
$\nu_5(b_{3g})$	132.5 (0)	132.2 (0)	135.3 (IR: 0, RA: 18)
$\nu_6(b_{3u})$	26.4 (0.1)	50.1 (0.1)	34.4 (IR:0.4, RA: 0)
Energy	–1405.08771	–1403.49167	
Energy including ZPVE	–1405.08502	–1403.48885	

Table 2. Comparison between the IR spectroscopic properties observed and calculated for $Al(\mu\text{-}Cl)_2Cl$ in three different isotopic forms [wavenumbers in cm^{-1}, IR intensities (in $km\,mol^{-1}$) given in parenthesis].

	$Al(\mu\text{-}^{35}Cl)_2Al$		$Al(\mu\text{-}^{35}Cl)(\mu\text{-}^{37}Cl)Al$		$Al(\mu\text{-}^{37}Cl)_2Al$	
Assignment[a]	Exp.	Calcd.	Exp.	Calcd.	Exp.	Calcd.
$\nu_1(a_g)$	298.6	298.4 (0)	297.7	297.1 (0.3)	296.3	295.7 (0)
$\nu_2(a_g)$		164.0 (0)		162.5 (0)		160.9 (0)
$\nu_3(b_{1u})$	270.95	287.1 (311)	269.29	285.4 (307)	267.51	283.7 (304)
$\nu_4(b_{2u})$	267.24	277.8 (59)	265.70	276.1 (58)	264.54	274.5 (57)
$\nu_5(b_{3g})$		132.5 (0)		131.6 (0)		130.8 (0)
$\nu_6(b_{3u})$		26.4 (0.1)		26.2 (0.1)		26.0 (0.1)

[a] D_{2h} symmetry. In the case of $Al(\mu\text{-}^{35}Cl)(\mu\text{-}^{37}Cl)Al$, the symmetry is reduced to C_{2v}.

which is in good agreement with the results of the quantum chemical calculations.

$[AlCl]_3$

Calculations on the trimer have not been reported previously. Accordingly, quantum chemical calculations were first carried out for several possible structures. These included a six-membered ring in a planar (**I**) or folded (**II**) structure, and a structure with an Al_3 triangle and three terminal Al–Cl bonds with the Cl atoms either in the plane defined by the three Al atoms (**III**) or outside it (**IV**). Calculations on these four structures were carried out both with BP/SVP and with MP2/TZVPP. It turns out that none of these structures defines the global minimum on the potential energy hypersurface. Surprisingly, such a structure, **V**, features two terminal Al–Cl bonds, a bridging Cl atom, and an Al atom which is bound to two Al atoms, but not to a Cl atom. All five structures as calculated with MP2/TZVPP are shown in Figure 6. Table 3 includes the energies as calculated with BP/SVP and MP2/TZVPP, as well as some salient bond lengths and angles. According to the calculations, structures **I** and **III** do not define minima on the potential energy hypersurface, since the vibrational analysis yields imaginary frequencies. Deviations between the results of BP/SVP and MP2/TZVPP are generally small, the only exception arises in the case of structure **II**. The Al–Cl and Al–Al distances decrease steadily from structure **I** to structure **V**. At the same time, the energy also decreases.

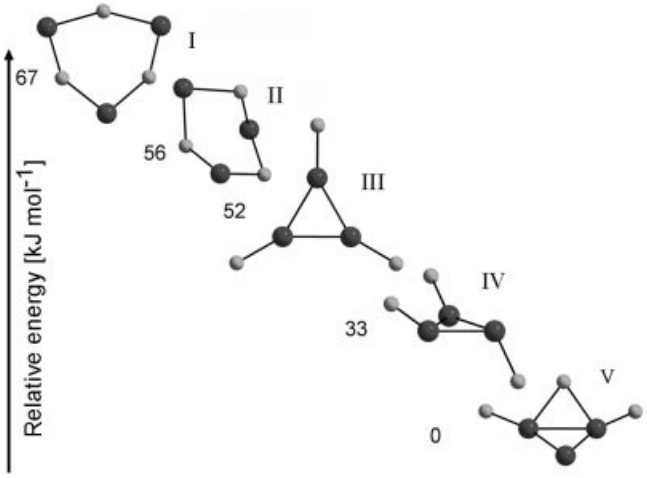

Figure 6. Possible structures of the trimer Al_3Cl_3 and their relative energies as calculated with MP2/TZVPP or BP/SVP.

Table 4 and Table 5 include the wavenumbers calculated for the vibrational modes of cyclic Al_3Cl_3 (structure **II**) and of Al_3Cl_3 in its C_s-symmetric energy minimum form (structure **V**). The mode of **V** which carries most of the IR intensity is located at 533.9 cm^{-1} [$\nu_8(a'')$] according to the calculations, which tallies very closely with the band near 530 cm^{-1} observed in the IR experiments. Although the observed band is weak, it shows evidence of a distinct isotopic pattern. In particular, there are three maxima at 531.3, 528.8 and 526.6 cm^{-1}; the band at 531.3 cm^{-1} carries most

Table 3. Energies (in hartree), distances (in pm) and angles (in °) as calculated for the different possible structures **I**–**V** of Al_3Cl_3 considered in this work (see Figure 6).

Method	Parameter	**I**[a]	**II**	**III**[a]	**IV**	**V**[b]
BP/SVP	Energy	–2107.63409	–2107.63439	–2107.63695	–2107.64390	–2107.65205
	Al–Cl	246	245–247	215	214–215	213/246 (Cl_b)
	Al···Al	466	454–457	275	268–282	260/280
	Al–Cl–Al	143	135–137			70 (Cl_b)
	Cl–Al–Cl	97	95			109 (Cl_b)
	Al–Al–Al			60	58–64	58–65
MP2/TZVPP	Energy	–2105.23646	–2105.24045	–2105.24199	–2105.24917	–2105.26183
	Al–Cl	244	238–258	212	212–214	211/240 (Cl_b)
	Al···Al	466	372–400	274	267–287	261/278
	Al–Cl–Al	146	100–103			71 (Cl_b)
	Cl–Al–Cl	94	84–91			107 (Cl_b)
	Al–Al–Al			60	58–65	58–65

[a] Structures **I** and **III** define no minima on the potential energy hypersurface since the vibrational analysis yields imaginary frequencies. [b] Cl_b means that the bridging Cl atom is considered.

of the intensity and that at 526.6 cm^{-1} is very weak. If this band indeed belongs to the trimer, it can be assigned to the antisymmetric ν(Al–Cl_t) mode. To simulate the isotopic pattern expected for the minimum energy structure, the wavenumbers for this mode have been calculated for all eight possible isotopomers ($^{35}Cl/^{37}Cl$). Isotopic substitution of the bridging Cl atom has, as anticipated, the smallest effect on the wavenumber of the mode. The $Al_3{}^{35}Cl_2(\mu\text{-}{}^{35}Cl)$ isotopomer has a wavenumber of 535.1 cm^{-1}. The $Al_3{}^{35}Cl_2(\mu\text{-}{}^{37}Cl)$ isotopomer has a corresponding wavenumber also of 535.1 cm^{-1}, and for the two $Al_3{}^{35}Cl^{36}Cl(\mu\text{-}{}^{35}Cl)$ isotopomers, a wavenumber of 532.5 cm^{-1} is found. In the case of two ^{37}Cl atoms and one ^{35}Cl atom in the molecule, a wavenumber of 532.5 cm^{-1} is found if the ^{35}Cl atom occupies a terminal position, while a wavenumber of 530.4 cm^{-1} results if the ^{35}Cl is in the bridging position. Finally, the $Al_3{}^{37}Cl_2(\mu\text{-}{}^{37}Cl)$ isotopomer is calculated to give a wavenumber of 530.4 cm^{-1}. In total, given the half width of the bands, an almost perfect triplet pattern results, which reveals distinct similarities between this and the observed pattern. The position and the isotopic pattern of the observed band is thus consistent with its belonging to the trimer Al_3Cl_3 in its C_s-symmetric energy minimum structure **V**.

In the case of the cyclic Al_3Cl_3 isomer, the mode with the highest wavenumber occurs at ca. 300 cm^{-1} according to the calculations (see Table 4). This implies that such a molecule cannot be responsible for the absorption at ca. 530 cm^{-1} detected in the IR experiment.

An alternative explanation for this band is that it represents the first overtone of the triplet at 267.24/265.70/264.54 cm^{-1} that belongs to Al_2Cl_2. The first overtone should occur at 534.5/531.4/529.1 cm^{-1} in the hypothetical case of zero anharmonicity. However, the wavenumber difference between the three resolved maxima observed within the band near 530 cm^{-1} (2.6 and 2.2 cm^{-1}) is somewhat smaller than that predicted for the overtone (3.1 and 2.3 cm^{-1}). Such an explanation is therefore less plausible. It is possible, on the other hand, that the overtone of the $\nu_3(b_{1u})$ and/or $\nu_4(b_{2u})$ mode of Al_2Cl_2 is responsible for the broader shoulder on the higher-wavenumber side of the band near 530 cm^{-1}. Unfortunately, because of the weak intensity, which also allows detection at very high AlCl concentrations in the matrix, Al_2Cl_2 cannot be distinguished with certainty from Al_3Cl_3 on the basis of intensity changes versus concentration in the matrix.

Table 4. Calculated vibrational properties (wavenumbers in cm^{-1}, IR intensities in $km\,mol^{-1}$ given in parentheses) and energy (in hartree) for cyclic Al_3Cl_3 (**II**).

	BP/SVP	MP2/TZVPP
ν_1	279.0 (310)	311.7 (57)
ν_2	278.0 (277)	296.1 (78)
ν_3	257.2 (7)	272.6 (231)
ν_4	253.7 (22)	248.6 (56)
ν_5	253.0 (17)	195.4 (91)
ν_6	142.8 (0.03)	185.3 (34)
ν_7	136.6 (0.003)	123.3 (2)
ν_8	82.9 (0.2)	98.8 (0.2)
ν_9	82.2 (0.2)	85.6 (11)
ν_{10}	58.2 (0.6)	53.3 (2)
ν_{11}	24.9 (0.03)	46.3 (0.004)
ν_{12}	3.4 (0.03)	39.9 (3)
Energy	–2107.63439	–2105.24045
Energy including ZPVE	–2107.63017	–2105.23599

Table 5. Calculated vibrational properties (wavenumbers in cm^{-1}, IR intensities in $km\,mol^{-1}$ given in parentheses) and energy (in hartree) for Al_3Cl_3 (C_s symmetry, **V**).

	BP/SVP	MP2/TZVPP
ν_1 (a′)	559.9 (79)	581.5 (98)
ν_2 (a′)	337.7 (61)	357.3 (78)
ν_3 (a′)	276.6 (20)	283.9 (23)
ν_4 (a′)	195.8 (2)	214.5 (3)
ν_5 (a′)	94.8 (1)	106.2 (0.3)
ν_6 (a′)	90.3 (1)	100.2 (3)
ν_7 (a′)	41.2 (1)	45.8 (1)
ν_8 (a″)	533.9 (181)	552.5 (223)
ν_9 (a″)	230.8 (8)	246.7 (9)
ν_{10} (a″)	121.0 (2)	149.6 (7)
ν_{11} (a″)	117.3 (1)	119.9 (0.5)
ν_{12} (a″)	92.1 (2)	102.2 (2)
Energy	–2107.65205	–2105.26183
Energy including ZPVE	–2107.64593	–2105.25531

In comparison with the neutral Al_3R_3 species, there is a higher chance of stabilizing radical anions with the formula $[Al_3R_3]^{\cdot-}$. R should be a sterically demanding group, e.g. $Si(SiMe_3)_3$. Calculations were carried out to determine the possible structures of these species. Figure 7 shows two possible isomers in the case of R = SiH_3, which have been optimized with BP/TZVPP. It turns out that the minimum energy structure again features two terminal Al–Si bonds and a bridging SiH_3 group. Again, the metal atoms form a triangle, and one of the metal atoms is bound directly only to other metal atoms, but not to a silyl group. A structure in which all metal atoms are bound to one silyl group exhibits a slightly higher energy (+10 kJ mol^{-1}). Anions of the form $[Al_3R_4]^-$ are already known, but in those cases, two of the metal atoms are bound to one ligand, and the third metal atom, to two ligands (R = Si*t*Bu$_3$).[23]

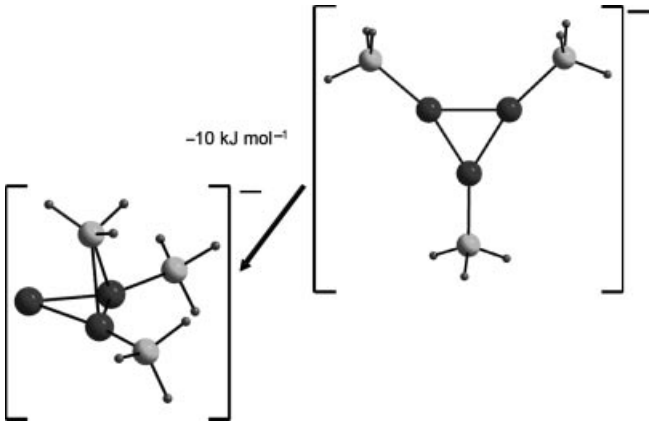

Figure 7. Calculated structures and relative energies for two isomers of $[Al_3(SiH_3)_3]^-$ (BP/TZVPP).

The formal oxidation states of the Al atoms in the minimum energy structure calculated for $(AlCl)_3$ vary. The structure might therefore be described as an intermediate on the way to disproportionation. The results presented herein might be of importance for a better understanding of the disproportionation mechanism.

$[AlCl]_4$

As already mentioned, the structure of the tetramer has already been evaluated before by quantum chemical calculations.[10,24] The molecule exhibits T_d symmetry, with Al–Cl and Al···Al distances (210.9 and 263.9 pm, respectively) that are in good agreement with those calculated previously.[24] Unfortunately, all attempts to gain experimental access to Al_4Cl_4 have so far failed. However, the compound $[AlC_5(CH_3)_5]_4$, featuring also an Al_4 tetrahedron, has been synthesized and structurally characterized.[25] There are also other known representatives of molecules with the overall formula Al_4R_4 [e.g. R = $Si(SiMe_3)_3$[26] or $N(SiMe_3)(2,6\text{-}iPr_2C_6H_3N(SiMe_3)$[27]].

Oligomerization Pathway and Thermodynamic Considerations

The dimerization of AlCl to the cyclic $[AlCl]_2$ dimer is associated with an energy change of –48 kJ mol^{-1} (–46 kJ mol^{-1} including ZPVE corrections) according to calculations with BP/SVP, and of –39 kJ mol^{-1} (–38 kJ mol^{-1} including ZPVE corrections) according to calculations based on MP2/TZVPP.

The question arises of whether the Al_2Cl_2 observed in the IR and Raman spectra is already formed in the gas phase or in the course of a reaction between two AlCl monomers either during or after deposition of the matrix. The relative intensities of the bands belonging to AlCl and to Al_2Cl_2 vary (a) with the rate of HCl which is passed over the aluminum within the Knudsen cell, and (b) with the rate of argon deposition. These findings indicate that most of the Al_2Cl_2 is formed during or after deposition of the matrix and not in the gas phase. However, it is difficult to guarantee exactly identical conditions in the experiments. To answer this question in a more quantitative way, therefore, the intensities of the bands observed in the IR spectrum were first used in combination with the calculated relative intensities to estimate the relative concentration of AlCl and Al_2Cl_2 in the matrix. This gives a ratio AlCl:Al_2Cl_2 of ca. 11:1 in the case of the representative experiment for which the IR spectrum is shown in Figure 2. In the next step, the calculations are used to estimate the equilibrium concentrations of the monomer and dimer in the gas phase. In Figure 8, ΔG for the dimerization reaction is shown as a function of temperature for two different pressures. At a pressure of 10^{-5} mbar and a temperature of 1300 K (conditions typical of a matrix isolation experiment), ΔG is estimated to be +296 kJ mol^{-1}. Accordingly, there is no significant partial pressure of dimer in the gas phase under these conditions. The dimer must therefore be formed almost exclusively either during or after deposition of the matrix. For this pressure, negative ΔG values can be realized only at a temperature below ca. 150 K. In the case of a total pressure of 1 bar, negative ΔG values can be expected up to temperature of ca. 350 K. At these low temperatures, however, AlCl is not stable, since disproportionation to Al and $AlCl_3$ occurs.

The fact that dimerization occurs during or after matrix deposition at very low temperature implies that the activation barrier to this reaction is close to zero. As two electrons in the σ orbital are mainly centered on the Al atom,[17] AlCl resembles silylene, SiH_2. It has been shown that dimerization of SiH_2 (with a $^1A_1$ ground electronic state) along a "least-motion path" to give H_2SiSiH_2 (either in its C_{2h}-energy minimum structure or in the ethylene-like form with D_{2h} symmetry) is symmetry forbidden and opposed by a substantial barrier due to "avoided crossing".[28] On the other hand, dimerization on a "non-least-motion" with low symmetry is possible without a barrier. Although the exact pathway for the dimerization of AlCl has still to be investigated, it is certain that the symmetry has to change during the approach of the two AlCl fragments, and the chances

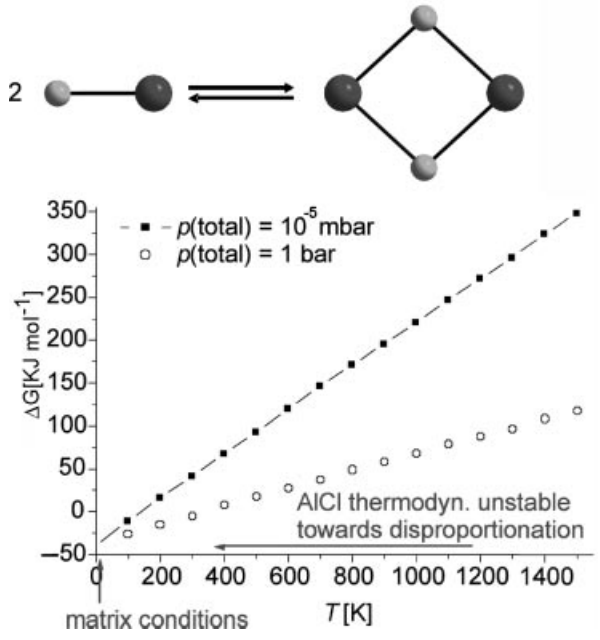

Figure 8. Dependence of ΔG on the temperature at 1 bar and 10^{-5} mbar total pressure for the dimerization of AlCl. Note that AlCl is thermodynamically not stable for temperatures below ca. 1200 K due to disproportionation into Al metal and $AlCl_3$.

of a pathway which includes a symmetry-restricted barrier are reduced. What seems clear, though, is that there is no significant barrier to dimerization.

The reaction of Al_2Cl_2 with another AlCl monomer to give Al_3Cl_3 in its C_s-symmetric energy minimum structure is also calculated to be exothermic. According to BP/SVP, the reaction energy is –78 kJ mol^{-1} without, and –71 kJ mol^{-1} with the inclusion of ZPVE corrections. By using MP2/TZVPP, the values are –84 kJ mol^{-1} without and –77 kJ mol^{-1} with the inclusion of ZPVE corrections. As expected, AlCl is therefore prone to oligomerization. Only at high temperatures do the significant entropy contributions to the Gibbs energy act to reverse this tendency.

Finally, formation of the Al_4Cl_4 tetramer from Al_3Cl_3 and AlCl is associated with an energy change of –218 kJ mol^{-1} (–211 kJ mol^{-1} with ZPVE corrections) at the BP/SVP level, and of –250 kJ mol^{-1} (–243 kJ mol^{-1} with ZPVE corrections) at the MP2/TZVPP level. Overall, the tetramerization energy for AlCl is –358 kJ mol^{-1} at the MP2/TZVPP level and with inclusion of ZPVE corrections. This value is in very good agreement with earlier estimates.[24]

Conclusions

The present studies draw on a combination of experimental and quantum chemical results to explore the oligomerization of AlCl monomers. Dimerization leads to cyclic, D_{2h}-symmetric Al_2Cl_2. This species isolated in an Ar matrix has been characterized in more detail by higher-resolution IR and Raman measurements. An evaluation of the thermodynamics of dimerization shows that the dimer cannot be present in significant amounts in the gas phase. The Gibbs energy change is negative only at low temperatures (but depends critically on the pressure), but at these low temperatures AlCl is thermodynamically unstable toward disproportionation into Al metal and $AlCl_3$. It follows that matrix isolation is the best method for gaining access to the dimer and higher oligomers. An isotopically structured, weak band in the IR spectrum of matrix-isolated AlCl has been assigned to the trimer Al_3Cl_3. This has a surprising structure, consisting of an Al_3 triangle with two terminal Al–Cl bonds and one Al–Cl–Al bridge; one of the Al atoms is directly bound to the other two metal atoms, but not to any of the Cl atoms. Thus, the formal oxidation states of the Al atoms vary. This might shed light on the disproportionation mechanism. Other possible structures have also been calculated, but exhibit a significantly higher energy. Quantum chemical calculations on the tetramer Al_4Cl_4 predict a molecule containing a tetrahedral Al_4 unit, in line with previous theoretical studies.

The results discussed here are of importance for a better understanding of the possible structures of not only solid AlCl but also the solvated species which have been exploited as a starting reagent for the synthesis of cluster compounds.[1] Figure 9 summarizes the oligomerization process and the calculated reaction energies of the relevant steps. It can be seen that the reaction energy is increasingly exothermal for each step.

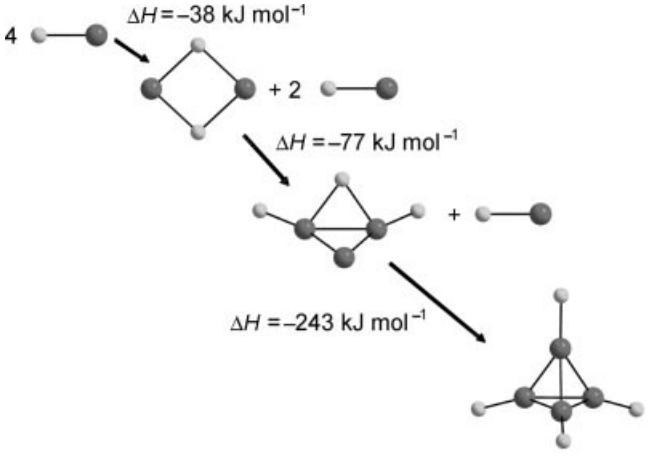

Figure 9. Reaction sequence leading from AlCl monomers via dimers and trimers to the Al_4Cl_4 tetramer. Reaction energies (MP2/TZVPP level, including ZPVE corrections) are given for each of the reactions in this sequence.

Experimental Section

In a resistively heated oven attached to a high vacuum apparatus, HCl was passed over liquid Al at a temperature of 1250 K. The AlCl thus generated was deposited together with excess Ar on a freshly polished Cu block kept at 12 K by means of a closed-cycle refrigerator (Leybold, LB115). Details of the matrix isolation technique can be found elsewhere.[29]

IR spectra were recorded with a Bruker 113v spectrometer equipped with an MCT detector, a DTGS detector, or a bolometer for measurements in the spectral region 4000–650, 700–200, or 700–30 cm^{-1}, respectively. The spectra were recorded with a resolution of 0.1 cm^{-1}.

Raman spectra were recorded with a Jobin Yvon XY spectrometer equipped with a pre-monochromator with two grids, a spectrograph and a CCD detector (Wright Instruments, England). The spectra were excited with the 514 nm line of an Ar^+ ion laser. The resolution was 0.5 cm^{-1}.

Quantum chemical calculations were carried out with the TURBOMOLE program package.[30] DFT (BP) as well as ab initio (MP2) methods were used in combination with SVP and TZVPP basis sets.

Acknowledgments

Financial support from the *Deutsche Forschungsgemeinschaft* and the *Fonds der Chemischen Industrie* is gratefully acknowledged.

[1] C. Dohmeier, D. Loos, H. Schnöckel, *Angew. Chem. Int. Ed. Engl.* **1996**, *35*, 129.
[2] K. P. Huber, G. Herzberg, *Molecular Spectra and Molecular Structure. IV. Constants of Diatomic Molecules*, van Nostrand Reinhold, New York, **1979**.
[3] A. Fontijn P. M. Futerko, *J. Phys. Chem.* **1993**, *97*, 7222.
[4] D. V. Dearden, R. D. Johnson III, J. W. Hudgens, *J. Chem. Phys.* **1993**, *99*, 7521.
[5] a) D. R. Lide Jr., *J. Chem. Phys.* **1965**, *42*, 1013; b) F. C. Wyse, W. Gordy, *J. Chem. Phys.* **1972**, *56*, 2130.
[6] H. Schnöckel, *Z. Naturforschung B* **1976**, *31*, 1291.
[7] a) H. Schnöckel, *J. Mol. Struct.* **1978**, *50*, 267; b) H. Schnöckel, *J. Mol. Struct.* **1978**, *50*, 275.
[8] M. Tacke, H. Schnöckel, *Inorg. Chem.* **1989**, *28*, 2895.
[9] See, for example: a) A. Schnepf, H. Schnöckel, *Angew. Chem. Int. Ed.* **2002**, *41*, 3533; b) H. Schnöckel, H. Köhnlein, *Polyhedron* **2002**, *21*, 489; c) H. Schnöckel, A. Schnepf, *Adv. Organomet. Chem.* **2001**, *47*, 235; d) G. Linti, H. Schnöckel, *Coord. Chem. Rev.* **2000**, *206–207*, 285.
[10] J. Gauss, U. Schneider, R. Ahlrichs, C. Dohmeier, H. Schnöckel, *J. Am. Chem. Soc.* **1993**, *115*, 2402.
[11] a) J. Bahlo, H.-J. Himmel, H. Schnöckel, *Angew. Chem. Int. Ed.* **2001**, *40*, 4696; b) J. Bahlo, H.-J. Himmel, H. Schnöckel, *Inorg. Chem.* **2002**, *41*, 2678; c) J. Bahlo, H.-J. Himmel, H. Schnöckel, *Inorg. Chem.* **2002**, *41*, 4488.
[12] H. Schnöckel, *J. Mol. Struct.* **1978**, *50*, 267.
[13] H.-J. Himmel, *Eur. J. Inorg. Chem.* **2003**, 4087.
[14] H.-J. Himmel, C. Klaus, *Z. Anorg. Allg. Chem.* **2003**, *629*, 1477.
[15] H.-J. Himmel, *Organometallics* **2003**, *22*, 2679.
[16] H.-J. Himmel, J. Bahlo, M. Haußmann, F. Kurth, G. Stößer, H. Schnöckel, *Inorg. Chem.* **2002**, *41*, 4952.
[17] H.-J. Himmel, *J. Chem. Soc. Dalton Trans.* **2002**, 2678.
[18] a) V. G. Solomonik, *Zhurnal Fizicheskoi Khimii* **1979**, *53*, 552; b) N. C. Baird, *Canadian J. Chem.* **1985**, *63*, 71.
[19] S. Petrie, *J. Phys. Chem. A* **1998**, *102*, 7828.
[20] M. D. Allendorf, C. F. Melius, B. Cosic, A. Fontijn, *J. Phys. Chem. A* **2002**, *106*, 2629.
[21] H.-J. Himmel, A. J. Downs, T. M. Greene, *J. Am. Chem. Soc.* **2000**, *122*, 922.
[22] See, for example: H. Schnöckel, S. Schnunck, T. Mehner, H. S. Plitt, *J. Am. Chem. Soc.* **1989**, *111*, 4578.
[23] N. Wiberg, T. Blank, W. Kaim, B. Schwederski, G. Linti, *Eur. J. Inorg. Chem.* **2000**, *7*, 1475.
[24] R. Ahlrichs, M. Ehrig, H. Horn, *Chem. Phys. Lett.* **1991**, *183*, 227.
[25] C. Dohmeier, C. Robl, M. Tacke, H. Schnöckel, *Angew. Chem. Int. Ed. Engl.* **1991**, *30*, 564.
[26] A. Purath, H. Schnöckel, *J. Organomet. Chem.* **1999**, *579*, 373.
[27] M. Schiefer, N. D. Reddy, H. W. Roesky, D. Vidovic, *Organometallics* **2003**, *22*, 3637.
[28] K. Ohta, E. R. Davidson, K. Morokuma, *J. Am. Chem. Soc.* **1985**, *107*, 3466.
[29] H.-J. Himmel, A. J. Downs, T. M. Greene, *Chem. Rev.* **2002**, *102*, 4191.
[30] a) R. Ahlrichs, M. Bär, M. Häser, H. Horn, C. Kölmel, *Chem. Phys. Lett.* **1989**, *162*, 165; b) K. Eichkorn, O. Treutler, H. Öhm, M. Häser, R. Ahlrichs, *Chem. Phys. Lett.* **1995**, *240*, 283; c) K. Eichkorn, O. Treutler, H. Öhm, M. Häser, R. Ahlrichs, *Chem. Phys. Lett.* **1995**, *242*, 652; d) K. Eichkorn, F. Weigend, O. Treutler, R. Ahlrichs, *Theor. Chem. Acc.* **1997**, *97*, 119; e) F. Weigend, M. Häser, *Theor. Chem. Acc.* **1997**, *97*, 331; f) F. Weigend, M. Häser, H. Patzelt, R. Ahlrichs, *Chem. Phys. Lett.* **1998**, *294*, 143.

Received: December 10, 2004

